Friction-mediated flow and jamming in a two-dimensional silo with two exit orifices

Ashish V. Orpe[*]

Chemical Engineering and Process Development Division, CSIR-National Chemical Laboratory, Pune 411008, India
and Academy of Scientific and Innovative Research (AcSIR), Ghaziabad 201002, India

Pankaj Doshi[†]

Pfizer Inc., Groton, Connecticut 06340, USA

We show that the interparticle friction coefficient significantly influences the flow and jamming behavior of granular materials exiting through the orifice of a two-dimensional silo in the presence of another orifice located in its vicinity. The fluctuations emanating from a continuous flow through a larger orifice results in an intermittent flow through the smaller orifice consisting of sequential jamming and flowing events. The mean time duration of jammed and flow events, respectively, increase and decrease monotonically with increasing interparticle friction coefficient. The frequency of unjamming instances (n_u), however, shows a nonmonotonic behavior comprising an increase followed by a decrease with increasing friction coefficient. The decrease on either side of the maximum, then, represents a system moving progressively towards a permanently jammed or a permanently flowing state. The overall behavior shows a systematic dependence on the interorifice distance, which determines the strength of the fluctuations reaching the smaller orifice leading to unjamming instances. The probability distributions of jamming and flowing times are nearly similar for different combinations of friction coefficients and interorifice distances studied and, respectively, exhibit exponential and power-law tails.

I. INTRODUCTION

A dry granular material exiting from an hopper or a silo can jam abruptly and quite unpredictably on its own [1–4]. On the contrary, the same jammed orifice requires forced intervention in some form to unjam or reinitiate the flow. The occurrence of the former is due to a stable arch formed at the exit and is dependent on the critical ratio of the size of particles to the orifice size, which is well defined for a three-dimensional hopper [5], but not necessarily for a two-dimensional hopper [6]. The latter phenomena occurs due to independent forcing of some form, primarily directed toward breaking of the arch, viz., impinging of an air jet through the orifice or vibration of the silo or a hopper [7] or the presence of flow through a nearby additional orifice [8,9]. While jet impinging or system vibration form external means of forcing, the presence of another orifice represents internal forcing, i.e., the inherent flow characteristics of the silo, in the form of velocity fluctuations, fed onto itself to cause unjamming which can also lead to improved mixing [10].

The continual presence of such an independent parallel forcing results in an intermittent flow through the orifice (flow followed by jamming followed by flow and so on), which can vary from a continuous flow regime to a permanently jammed regime dependent on the propensity of the forcing, i.e., vibration intensity [7] or the distance between two orifices [8]. Within the intermittent flow regime, the distribution of the times during which orifice is flowing exhibits an exponential tail, while those corresponding to jammed state exhibits a power-law tail [7]. The former represents the characteristic of a random behavior and is also observed during the flow from an orifice even in the absence of any independent forcing [8,11]. The latter behavior is shown to comprise two different regimes depending on the value of the power-law exponent [7]. For values of exponents 2 and lower, the distributions comprise jammed events of increasingly longer durations separating two consecutive flowing events. The average jamming time is ill defined and increases with increase in the total experimental duration, eventually diverging over very long durations suggestive of an overall jammed state. However, the progressively increasing exponent value above 2 leads to an overall flowing state with well defined mean jamming time. The exponent value of 2, thus, corresponds to a jamming to flowing transition.

Interestingly, this value of the exponent of 2 is quite insensitive to the type of independent forcing and has been shown to be valid for a variety of systems ranging from those occurring naturally (e.g., movement of a crowd of pedestrians or animals through a narrow exit) or artificially (e.g., motion of an assembly of granular or colloidal particles through an orifice) [12–14]. The overall behavior can be qualitatively predicted using an empirical model based on the Langevin equation with vibrations mimicking the thermal fluctuations [15]. The different systems, albeit showing similar universal behavior for jamming-to-flow transition, can be thought of possessing different friction coefficient between constituent entities. This, apparent effective friction coefficient, can owe its origin to different material characteristics. Experimentally,

[*]av.orpe@ncl.res.in
[†]pankaj.doshi@pfizer.com

it has been shown recently that the (continuous) flow rate of granular material through a two orifice silo exhibits a qualitative change in its dependence on interorifice distance with increase in interparticle friction coefficient [16]. The continuous flow of such granular material draining through two orifices, located far apart from each other but at various distances from the side walls has been predicted very well using kinematic theory based arguments [17].

In this work, we strive to explore the jamming and flowing phenomena through the orifice of a silo for varying interparticle friction coefficients and for the independent forcing occurring through the second continuously flowing orifice using discrete element method (DEM) simulations. This forcing will, thus, depend on the flow through the second orifice, its proximity to the jammed or flowing orifice, and the transmission of this forcing though the bed of grains. In the next section, we describe the system and simulation details, followed by the results comprising primary causes of unjamming phenomena and the relevant characteristics of the jamming and flowing behavior.

II. METHODOLOGY

The DEM simulations methodology employed is the same as used previously [8,18] and the system geometry is nearly identical to that used in the previous work [8]. We provide only the relevant details over here. The simulations, carried out using the Large Atomic/Molecular Massively Parallel Simulator (LAMMPS), employ a Hookean force between two contacting particles which consists of a normal component ($\mathbf{F_n}$) and a tangential component ($\mathbf{F_t}$). Each of this force has two terms, a contact force and a damping force given as [19]

$$\mathbf{F_n} = \left(k_n \delta \mathbf{n} - \frac{\gamma_n \mathbf{v}_n}{2} \right), \tag{1}$$

$$\mathbf{F_t} = -\left(k_t \Delta \mathbf{s}_t + \frac{\gamma_t \mathbf{v}_t}{2} \right), \tag{2}$$

where $\mathbf{n}$ is the unit vector along the line connecting centers of two particles, and $\mathbf{v}_t$ and $\mathbf{v}_n$ are, respectively, the tangential and normal components of particle velocities. The normal damping term (γ_n) is chosen as $50\sqrt{g/d}$, while the tangential damping term (γ_t) is set as $\gamma_n/2$. The normal elastic constant (k_n) is chosen as $2 \times 10^6 \, mg/d$ while the tangential elastic constant (k_t) is set as $2/7 \, k_n$. The elastic constants represent a stiffer particle in accordance with previous studies [18,20]. $\Delta \mathbf{s}_t$ is the tangential displacement between two particles to satisfy the Coulomb yield criterion given by $\mathbf{F}_t = \mu \mathbf{F}_n$, where μ is the friction coefficient, varied from 0.001 to 0.5. In the above expressions, d is the particle diameter, g represents gravity acting in downward direction and the particles have unit density which yields the mass (m_p) of the particle as $4\pi(d/2)^3 m/3$ with a natural mass unit m. The natural time unit τ is given as $\sqrt{d/g}$ and the integration time step used in the simulation is $\delta t = 2.5 \times 10^{-5}$.

A two-dimensional rectangular, flat bottomed silo geometry of thickness $1d$ is employed in this work. The width of the silo is specified in terms of d and the silo is filled upto an approximate height of ($80–90d$), with d being the mean particle diameter with a polydispersity of 15%. The bottom surface is created using smaller particles ($0.1d$) to mimic a smooth
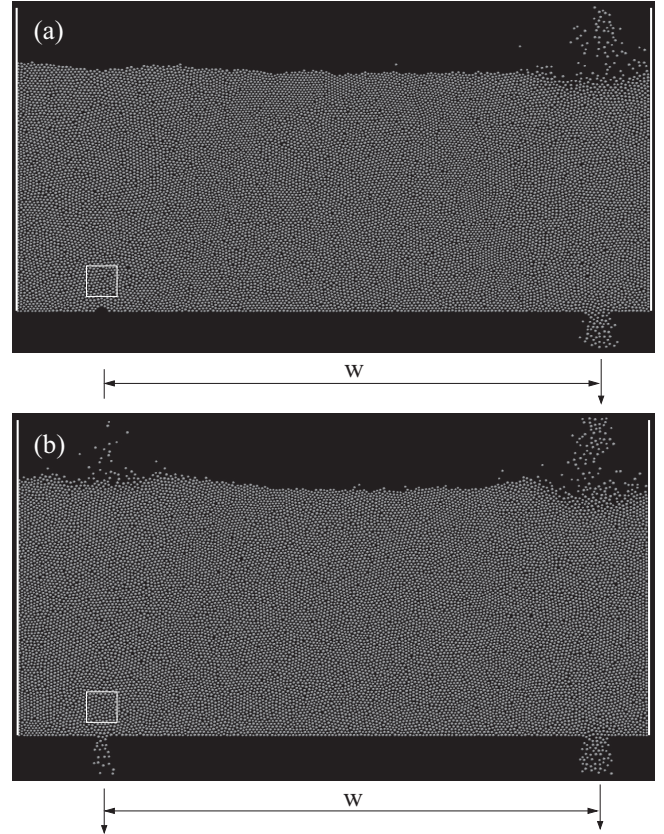

FIG. 1. Sample snapshots of the flow occurrence in a two-orifice silo for $w = 140d$. Flow occurs continuously through right orifice of width $8d$ while the left orifice (width $4d$) is jammed as shown in panel (a). The flow reinitialization occurring spontaneously through the left orifice at a later time is shown in panel (b). The white box ($10d \times 10d$) represents the region over which the time dependent mean velocity and average rms velocity is calculated. The white vertical lines represent the flat side walls. The pouring near the free surface represents the granular recirculation (see text for more details).

wall, which are kept frozen during the entire simulation run having zero translational and angular velocities. The flat side walls are created using the in-built function in LAMMPS. The friction coefficient between the flowing particles and both, the side and bottom, walls is maintained same as the interparticle coefficient. The simulation has two orifices of fixed widths ($D_1 = 8d$ and $D_2 = 4d$) separated by a distance w. The size of the larger orifice (D_1) was so chosen as to allow for continuous flow of particles throughout the simulation run. The silo width is maintained large enough for all w to prevent any sidewall effects. The silo is initially filled using the sedimentation method as suggested previously [20] in which a dilute packing of nonoverlapping particles is created in a simulation box and allowed to settle under the influence of gravity. The simulation is run for a significant time so that the kinetic energy per particle is less than $10^{-8} mgd$ resulting into a quiescent packing of desired fill height in the silo which defines the initial state.

Both the orifices are opened simultaneously to initiate the flow. The flow through larger orifice occurs continuously

without any interruption, while that through the smaller orifice shows intermittent flow: several successive sequences of flow and nonflow. Fig. 1(a) shows a sample snapshot of particles flowing through larger (right) orifice while the smaller (left) orifice is jammed. After a while, the flow restarts through the jammed orifice with continual flow through the larger orifice as shown in Fig. 1(b). The fill height (80–90d) is maintained constant by repouring the particles which exit the orifice, from a fixed distance above the free surface at the same horizontal location where they exited from the silo (see Fig. 1). Every simulation is executed for 500 million timesteps, which provides several jamming-unjamming sequences good enough to obtain meaningful averages. The total simulation time corresponds to that required by the particles to traverse the entire silo height at least 200 times. The snapshots of particle positions within the silo are saved at intervals of 0.25τ.

III. RESULTS AND DISCUSSION

The occurrence of flow through the smaller orifice ($D_2 = 4d$) can be represented in terms of instantaneous mean velocity (v) calculated inside the silo in a region $10d \times 10d$ centered at a position exactly $10d$ above the orifice and along the centerline through the orifice. The region is shown as white box in both the panels of Fig. 1. The mean velocity is defined as $v = \sqrt{\langle c_x \rangle^2 + \langle c_y \rangle^2}$. Here, c_x and c_y are, respectively, the instantaneous horizontal and vertical velocity components of every particle obtained from the displacements between two successive snapshots and $\langle . \rangle$ represents a spatial average over a region $10d \times 10d$ as defined above. The variation of mean velocity with simulation time is shown in Fig. 2 for one particular interorifice distance ($w = 140d$) and varying interparticle friction coefficients. A schematic similar to Fig. 2 has been presented previously [13] for a single orifice silo vibrated continuously at different intensities. The time t_j, depicted in the fourth panel, is defined as the time during which the left orifice remains jammed. Similarly, t_f, shown in second panel, is defined as the time during which the flow occurs through the left orifice before it gets jammed.

Several features, corresponding to jamming and flow occurrences in the silo, are evident from Fig. 2. The mean velocity value is zero at all times for $\mu = 0.5$ (top panel), which corresponds to the orifice remaining jammed at all times. A slight reduction in the interparticle friction coefficient ($\mu = 0.35$) shows few occurrences of sudden rise in the mean velocity, but only for a very brief time, followed by rapid decrease to zero velocity. These are seen as spikes emanating from zero velocity line as shown in second panel in Fig. 2. The orifice, thus, remains jammed throughout with occasional spurts of flow for a brief period of time. The mean, $\langle t_f \rangle$, is quite low for this case, while $\langle t_j \rangle$ is quite high. Here, $\langle . \rangle$ represents average over entire simulation run. The instances of flow re-initiation increase continuously with decreasing friction coefficient. Further, the duration of the flow following the unjamming event also increases continuously as evident from contiguous clusters of spikes. With a significant decrease in the friction coefficient ($\mu = 0.025$, panel five in Fig. 2), the situation gets reversed with the flow now occurring almost at all times with sudden occasional dips in the velocity to zero, for a brief period of
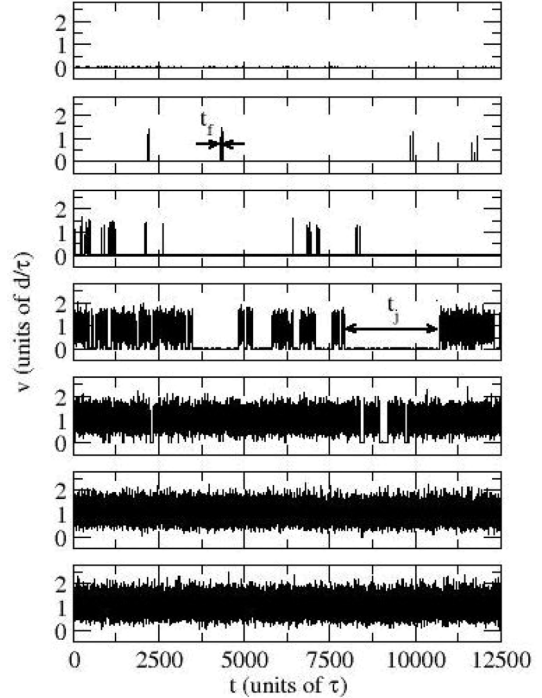

FIG. 2. Variation of mean velocity (v) of the flow with time (t) occurring through the left orifice shown in Fig. 1 for $w = 140d$. The values of friction coefficient (μ) vary from top panel to bottom panel as 0.5, 0.35, 0.1, 0.05, 0.025, 0.01, and 0.001, respectively. The time duration of flowing and jammed states are, respectively, represented by t_f and t_j.

time. In this case, the mean, $\langle t_f \rangle$, is quite high, while $\langle t_j \rangle$ is quite low. This scenario represents occasional jamming of orifice in an otherwise continuous flow. Decreasing the value of μ further eliminates these occasional jamming events as well leading to a continuous flow throughout (i.e., diverging $\langle t_f \rangle$). This behavior is exactly opposite to that observed for $\mu = 0.5$ (top panel), for which $\langle t_j \rangle$ diverges. Apparently, the state of the orifice shows a step change from presence of a continuous zero velocity to a continuous nonzero velocity of an approximate magnitude of $1.2d/\tau$. This nonzero velocity shows fluctuations about the mean, which are perhaps due to lack of smooth flow, possible only through an orifice of larger size, for instance, D_1. The overall behavior from one state to other through a transition is clearly due to the presence of continuous, smooth, steady flow occurring through right orifice ($D_1 = 8d$), in the absence of which, the jammed (left) orifice will not be able to unjam again [8]. The probable cause of this time dependent, friction-dependent and interorifice-dependent jamming-unjamming behavior is discussed next.

The velocity contours across the entire silo are obtained for all those times when the left orifice remains jammed. The mean velocity (v) at different locations is calculated using the expression mentioned above while the fluctuations of mean velocity are measured in terms of root-mean-squared (rms) velocity which is defined as $u = \sqrt{[\langle c_x^2 \rangle - \langle c_x \rangle^2] + [\langle c_y^2 \rangle - \langle c_y \rangle^2]}$. For both quantities, $\langle . \rangle$ represents the spatial average over a $3d \times 3d$ region and the
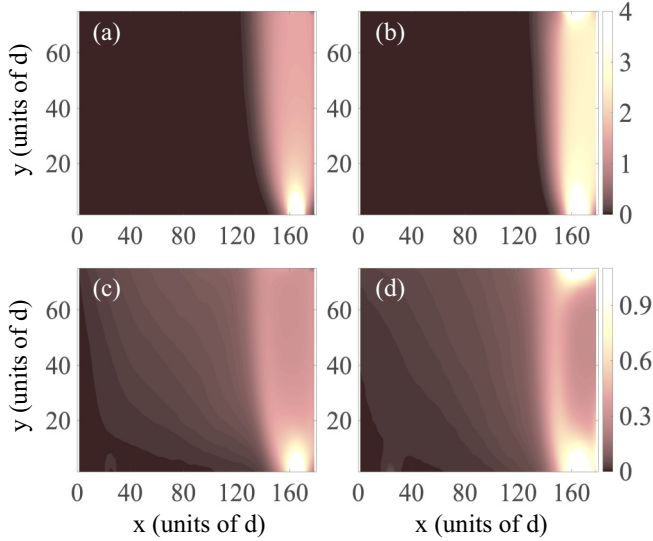
FIG. 3. Contour plot of velocities in the silo for an interorifice distance of $w = 140d$ and two different friction coefficients. The contours are obtained as averages over all those times when the left orifice at $x = 25d$ remains jammed while the flow occurs continuously through the right orifice at $x = 165d$. Mean velocity field for (a) $\mu = 0.35$ and (b) $\mu = 0.05$. RMS velocity field for (c) $\mu = 0.35$ and (d) $\mu = 0.05$. The scale (color bar) common to each row is shown on the extreme right.

FIG. 4. (a) Variation of the rms velocity (u) of the flow with friction coefficient (μ) for various interorifice distances (w). The value of u is measured in the white box shown in Fig. 1 and is obtained as an average over all times instances whenever the left orifice remains in the jammed state. (b) Variation of mean jammed duration $\langle t_j \rangle$ with friction coefficient (μ) for various interorifice distances (w).

temporal average over all the time instants whenever the left orifice is in a jammed state. The spatial region for averaging is chosen large enough to get better statistical averages, but is small enough to reasonably represent the contour map. The contour map for mean and rms velocity in the silo for an interorifice distance of 140d and for two different friction coefficients is shown in Fig. 3. Since the contours are obtained only for those times when the left orifice remains jammed, the observed spatial variation in the velocity magnitudes is the outcome of the continuous flow occurring through the right orifice located at $x = 165d$. The mean velocity has a nonzero magnitude only in a small vertical band ($x > 130d$) stretching from the orifice to the free surface. Elsewhere the mean velocity is close to zero. The unjamming of left orifice, located at $x = 25d$ and requiring slightest of relative motion between particles forming the arch, in that case does not seem to arise due to mean velocity field. Note that the change in the friction coefficient (even by an order of magnitude difference) does not seem to affect the spatial variation of mean velocity [Figs. 3(a) and 3(b)].

The rms velocity, however, shows a much broader spatial variation in the silo and seems to exhibit dependence on the friction coefficient [Figs. 3(c) and 3(d)]. For both, $\mu = 0.05$ and $\mu = 0.35$, the fluctuations are observed to be present almost everywhere in the system, which are expected to cause the relative motion of the particles in the arch leading to unjamming. The fluctuations do, however, show an increased spatial coverage for $\mu = 0.05$ when compared to those observed for $\mu = 0.35$, and they extend up to the jammed orifice in the former case. Increased tangential damping during particle-particle contacts is expected for increased friction
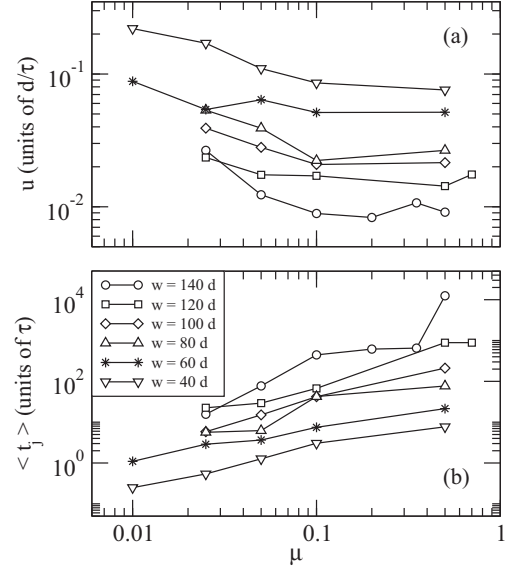
coefficient ($\mu = 0.35$) thereby weakening the fluctuations reaching the jammed orifice which are, thus, not evident in the figure scale. These weakening fluctuations may cause cumulative relative motion of particles in the arch, but over a much longer time duration, thereby increasing the duration of the jammed events (see Fig. 2, second panel), consequently higher $\langle t_j \rangle$. In the similar vein, the lower value of $\mu = 0.05$ will cause relatively stronger fluctuations to be present in the vicinity of the orifice, thereby causing the orifice to remain jammed for a smaller duration of time (see Fig. 2, fourth panel), consequently, lower $\langle t_j \rangle$. In the event of a very high friction coefficient ($\mu = 0.5$), the fluctuations reaching the left orifice are not of significant magnitude to cause unjamming even once over the entire simulation run (Fig. 2, first panel). It is to be noted that the unjamming of the left orifice occurs only when there is a flow through the right orifice. Few simulations without the presence of right orifice showed that the flow through left orifice, once jammed, does not unjam on its own even over timescales close to that for an entire simulation run. Similar qualitative behavior is also observed for other interorifice distances.

To quantify the effect of fluctuations on unjamming even further, we have calculated the rms velocity in a larger region ($10d \times 10d$), the same which was used for obtaining the time dependent velocities shown in Fig. 2. As earlier, the rms velocity is obtained as average over the region as well as over all durations whenever the left orifice is in the jammed state. The variation of rms velocity with friction coefficient for various interorifice distances is shown in Fig. 4(a). The rms velocity, shows some scatter, but decreases monotonically with increased friction coefficient and increasing interorifice distance. Both the trends are expected to arise out of higher

tangential damping during particle-particle contacts, thereby weakening the fluctuations in the vicinity of the jammed orifice originating from the continuous flow in the right orifice. A direct correlation of this effect is observed with the averaged duration of jammed states ($\langle t_j \rangle$) which increases monotonically with increased values of μ as well as w as shown in Fig. 4(b).

The overall effect of the fluctuations on the jamming-unjamming behavior of the orifice observed over here is somewhat analogous to that observed previously for single orifice silos. The fluctuations drivers in friction coefficient and the interorifice distance, then, correspond to the intensity of vibrations employed for a dry granular system [7] or the variation of temperature for a colloidal system [14] or some random force causing the pedestrians to exit from a bottleneck [12]. Such fluctuation driven flow, also known as nonlocal flow, has been studied previously in different geometries and under different flow conditions [21,22]. It has been shown that the localised shear gives rise to stress fluctuations leading the material to yield and flow elsewhere [21] akin to a self-activated process. This nonlocal flow has been expressed adequately using appropriate constitutive equations for the relevant rheology [23].

We next discuss the kinematics of jamming and unjamming events. The duration of every jammed and flow events is, respectively, represented by t_j and t_f as mentioned earlier. The frequency of unjamming (n_u) is defined as the number of times the orifice unjams over the entire simulation time period ($t = 12500\tau$). The values of t_j, t_f, n_u are obtained by monitoring the presence of particles in the outflow from the left orifice and the averages $\langle . \rangle$ are obtained over the entire simulation duration. The variation of n_u, $\langle t_j \rangle$, and $\langle t_f \rangle$ with friction coefficient (μ) for different interorifice distances (w) employed is shown in Fig. 5.

The effect of friction coefficient (μ) for a fixed value of w is discussed first followed by the overall dependence on w. Consider the profiles for $w = 140d$ shown in the topmost panel. Both, $\langle t_j \rangle$ shown as red solid lines and $\langle t_f \rangle$ shown as blue dashed lines, show a monotonic dependence on the friction coefficient, though in opposite direction. The average time over which the orifice remains jammed, increases progressively with increased value of μ, while the average time for which the orifice is flowing, decreases progressively. As discussed earlier with respect to Figs. 3 and 4, the increased friction leads to weaker fluctuations reaching the orifice thereby allowing for longer duration of the arch (i.e., jammed state) before causing slight rearrangements leading to unjamming. The curves for $\langle t_j \rangle$ and $\langle t_f \rangle$ cross each other at some value of crossover friction coefficient, denoted as μ_c, for which the average duration of jammed and flowing states are identical, for instance, a situation similar to that shown in panel 4 in Fig. 2.

The frequency of unjamming occurrences, however, shows a nonmonotonic dependence on the value of μ, with the maximum occurring quite close to μ_c where the curves for jamming and flowing times intersect. On either side of the maximum, identical value of frequency is achievable for two different values of μ, though the origin is quite opposite to each other. Towards the left side, for smaller values of μ, the orifice remains in the flowing state for most of the
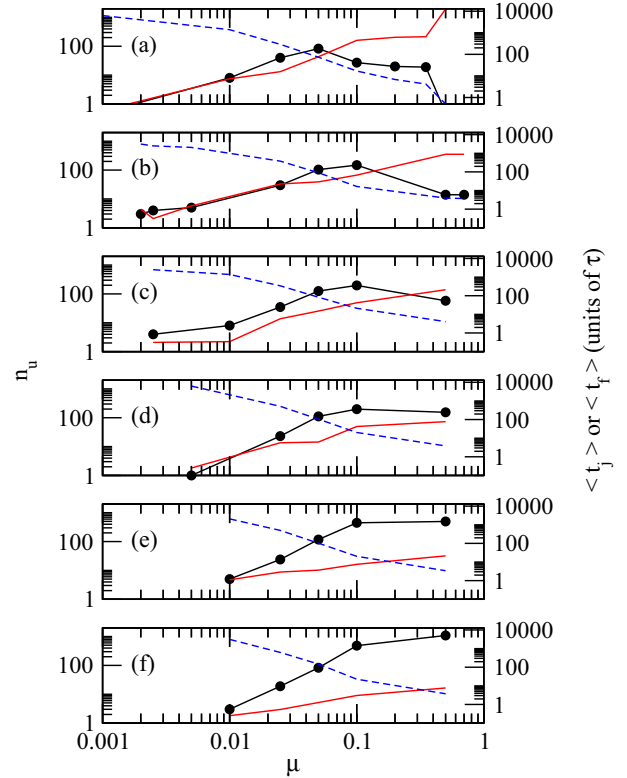

FIG. 5. Variation of mean jammed duration $\langle t_j \rangle$ (solid, red lines), mean flow duration $\langle t_f \rangle$ (dashed, blue lines) and the frequency of unjamming n_u (lines with filled circles) with friction coefficient (μ). The data is shown for different interorifice distances, namely, (a) $w = 140d$, (b) $w = 120d$, (c) $w = 100d$, (d) $w = 80d$, (e) $w = 60d$, and (f) $w = 40d$.

time with few jamming events, consequently lesser number of unjamming instances and hence lower n_u. The smaller value of n_u on the right side is also the result of lesser number of unjamming events, but due to the orifice remaining jammed for a longer duration due to weaker fluctuations reaching the jammed orifice. The value of n_u eventually reaches zero for very small and very high friction coefficients, which represents, respectively, a completely jammed state (first panel in Fig. 2 and diverging $\langle t_j \rangle$) and a completely flowing state (last panel in Fig. 2 and diverging $\langle t_f \rangle$). The friction coefficient (nearly same as μ_c) corresponding to the maximum in the frequency curves, can then, perhaps, be termed as the flowing-jamming transition point. The variation in the value of μ, either decreasing below or increasing above μ_c, shifts the system, respectively, towards either a progressively flowing or a progressively jammed state.

A similar behavior was observed previously by Janda *et al.* [7] in an experimental study on vibrated silo with a single orifice. The average jamming time showed a progressive decrease with an increase in the vibrational intensity. The progressive, smooth decrease, however, was shown to transform to a step curve around a critical vibrational intensity bifurcating the jammed and flowing states, if the silo was allowed to flow for an infinitely long duration of time. The analog of the critical vibrational intensity in the present case

is the crossover friction coefficient μ_c corresponding to the maximum frequency.

The overall behavior of $\langle t_j \rangle$, $\langle t_f \rangle$, and n_u is preserved qualitatively for decreasing interorifice distances as shown in the remaining panels of Fig. 5, but with quantitative differences. The value of crossover or transition μ_c increases with decreasing interorifice distance. This means that for a fixed value of μ, the jamming dominated regime is obtained for larger interorifice distance, while flowing dominated regime is obtained at smaller interorifice distance. For instance, the same fluctuations originating from the same right orifice for $\mu = 0.2$, are weak enough to cause unjamming of the other orifice situated $140d$ away, but are significantly strong enough to cause frequent unjamming of the second orifice situated only $40d$ away. The jamming to flowing transition (μ_c), if as defined, does not seem to be unique, but is a function of the interorifice distance which also serves to induce independent forcing in the system. The values of average jamming and flowing times at crossover or transition point are significantly reduced at smaller w showing relatively rapid occurrences of jamming and unjamming instances. The reason for this being the progressively stronger fluctuations available at the jamming/unjamming orifice with decreasing values of w. Not surprisingly, the values of n_u become higher at the crossover friction coefficient with decreasing w. While the curves for $w = 80d$ and lower are incomplete towards higher friction coefficients, they nevertheless convey the same qualitative behavior. The relative flattening of the frequency curves at higher values of μ, but for smaller values of w, cannot be commented due to inadequate data available.

The distributions of jamming times (t_j) and flowing times (t_f), normalized by their respective mean values are shown in Fig. 6 for four different friction coefficients and various interorifice distances. The distributions for both cases seem to show similar behavior across μ and w employed, albeit with a larger scatter in the distributions for the unjamming times as well as deviations in the tails in few of the cases. The distribution of the flowing time shows an exponential behavior [dashed line in Fig. 6(a)] for all combinations of w and μ, except one or two cases. The exponential behavior is typical of the random nature of discrete avalanche events and is in accordance with the behavior observed previously for single [7,11] as well as multiorifice [8] silos. The occurrence of jamming, thus, is not necessarily influenced by the presence of independent forcing in the form of fluctuations originating from the second orifice in the system. The occurrence of unjamming is, however, clearly dependent on the presence of second orifice and the fluctuations generated therein. The distributions of jamming times, thus, do not show an exponential behavior, but seem to exhibit a power-law behavior with an exponent value of 2 across the data for most of the combinations of w and μ studied. Previous studies using single orifice silo with varying independent forcing have also observed power-law tail in the distributions for the unjamming times [7,12,13]. The exponent value of two was shown to be closely related to jamming-flowing transition, with values greater than two dominated by flowing occurrences, while those equal or lower than two dominated by jamming occurrences.
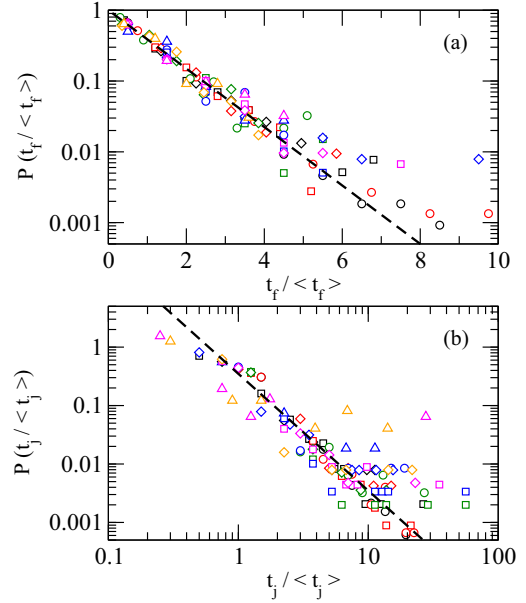

FIG. 6. Probability distribution of (a) normalized flow time (t_f) and (b) normalised jammed time (t_j) obtained for various interorifice distances and friction coefficients. Data is represented by ○ ($\mu = 0.5$), □ ($\mu = 0.1$), ◇ ($\mu = 0.05$) and △ ($\mu = 0.025$). The color of the symbol represents different values of interorifice distances: black ($w = 40d$), red ($w = 60d$), green ($w = 80d$), blue ($w = 100d$), magenta ($w = 120d$), and orange ($w = 140d$). The dashed line in (a) represents an exponential fit while the dashed line in (b) represents a power-law fit with an exponent of 2. See text for more details.

IV. SUMMARY

The jamming and flowing behavior of granular material exiting through a narrow orifice is investigated in the presence of another continuously flowing wide orifice located in the vicinity for varying interparticle friction coefficients. Intermittent flow, consisting of sequential jammed and flowing events, is observed to occur through the smaller orifice. The mean time duration of jammed events increases monotonically with increasing friction coefficients, eventually diverging at very high friction coefficient resulting in a permanently jammed state. The opposite behavior is observed for the mean time duration of flowing events which exhibits a permanently flowing state at small enough friction coefficient. The friction coefficient manifests itself by influencing the magnitude of the intensity of fluctuations reaching the narrow orifice arising out of several interparticle contact interactions in the system leading to an intermittent flow.

The frequency of the unjammed events (n_u) exhibits a nonmonotonic behavior comprising a gradual increase followed by a gradual decrease with increasing value of friction coefficient. The crossover friction coefficient μ_c corresponding to the maximum in the value of n_u can be thought to be as jamming-to-flowing transition point. A progressive decrease below or increase above μ_c, respectively, shifts the system monotonically towards progressively increased duration of flowing or jammed events. The value of μ_c shifts towards higher values for decreasing interorifice distances accompanied by progressively increasing corresponding frequency

values. The distributions of flowing time durations exhibit an exponential tail in accordance with a typical randomly occurring event independent of the induced forcing. The distributions for the jammed duration, however, show a slower power-law decay and a definite dependence on the induced forcing.

The interparticle friction coefficient governs the momentum transfer between contacting particles causing them to move either slowly or faster. Its variation, in principle, can be considered to represent varying momentum transfer through different modes of independent forcing incorporated previously to study unjamming, ranging from dry granular material [7] through colloidal suspensions [13] to motion of self-propelled vehicles [24] and living agents [12] across narrow constrictions. This inference which is obviously valid in the absence of any other mechanism governing momentum transfer, for instance collision in granular system, nevertheless provides a more generic nature to the observed behavior in this work. More interesting would be to study the effect of friction on jamming-unjamming behavior in tilted silos [25–27] which provides tilt angle as another controlling parameter and for more practical cohesive systems which provides altered lengthscale to account for cluster size instead of single particle size.

[1] K. To, P. Y. Lai, and H. K. Pak, Phys. Rev. Lett. **86**, 71 (2001).

[2] J. Tang and R. P. Behringer, Chaos **21**, 041107 (2011).

[3] S. Tewari, M. Dichter, and B. Chakraborty, Soft Matter **9**, 5016 (2013).

[4] I. Zuriguel, Pap. Phys. **6**, 060014 (2014).

[5] I. Zuriguel, L. A. Pugnaloni, A. Garcimartín, and D. Maza, Phys. Rev. E **68**, 030301(R) (2003).

[6] A. Janda, I. Zuriguel, A. Garcimartín, A. Pugnaloni, and D. Maza, Eur. Phys. Lett. **84**, 44002 (2008).

[7] A. Janda, D. Maza, A. Garcimartín, E. Kolb, J. Lanuze, and E. Clément, Eur. Phys. Lett. **87**, 24002 (2009).

[8] A. Kunte, P. Doshi, and A. V. Orpe, Phys. Rev. E **90**, 020201(R) (2014).

[9] S. Mondal and M. M. Sharma, Granular Matter **16**, 125 (2014).

[10] S. Kamath, A. Kunte, P. Doshi, and A. V. Orpe, Phys. Rev. E **90**, 062206 (2014).

[11] I. Zuriguel, A. Janda, A. Garcimartín, C. Lozano, R. Arévalo, and D. Maza, Phys. Rev. Lett. **107**, 278001 (2011).

[12] I. Zuriguel, D. R. Parisi, R. C. Hidalgo, C. Lozano, A. Janda, P. A. Gago, J. P. Peralta, L. M. Ferrer, L. A. Pugnaloni, E. Clément, D. Maza, I. Pagonabarraga, and A. Garcimartín, Sci. Rep. **4**, 7324 (2014).

[13] I. Zuriguel, A. Janda, R. Arévalo, D. Maza, and A. Garcimartín, EPJ Web. Conf. **140**, 01002 (2017).

[14] R. C. Hidalgo, A. Goñi-Arana, A. Hernández-Puerta, and I. Pagonabarraga, Phys. Rev. E **97**, 012611 (2018).

[15] A. Nicolas, A. Garcimartín, and I. Zuriguel, Phys. Rev. Lett. **120**, 198002 (2018).

[16] L. A. Fullard, E. C. P. Breard, C. E. Davies, A. J. R. Godfrey, M. Fukuoka, A. Wade, J. Dufek, and G. Lube, Proc. R. Soc. A **475**, 20180462 (2019).

[17] R. Maiti, G. Das, and P. K. Das, Phys. Fluids **29**, 103303 (2017).

[18] C. H. Rycroft, A. V. Orpe, and A. Kudrolli, Phys. Rev. E **80**, 031305 (2009).

[19] http://lammps.sandia.gov/.

[20] J. W. Landry, G. S. Grest, L. E. Silbert, and S. J. Plimpton, Phys. Rev. E **67**, 041303 (2003).

[21] K. A. Reddy, Y. Forterre, and O. Pouliquen, Phys. Rev. Lett. **106**, 108301 (2011).

[22] K. Nichol and M. van Hecke, Phys. Rev. E **85**, 061309 (2012).

[23] K. Kamrin and G. Koval, Phys. Rev. Lett. **108**, 178301 (2012).

[24] G. A. Patterson, P. I. Fierens, F. S. Jimka, P. G. König, A. Garcimartín, I. Zuriguel, L. A. Pugnaloni, and D. R. Parisi, Phys. Rev. Lett. **119**, 248301 (2017).

[25] C. C. Thomas and D. J. Durian, Phys. Rev. E **87**, 052201 (2013).

[26] C. C. Thomas and D. J. Durian, Phys. Rev. Lett. **114**, 178001 (2015).

[27] C. C. Thomas and D. J. Durian, Phys. Rev. E **94**, 022901 (2016).